

# The Effect of Load and Abrasive Particle Size on the Material Removal Rate of Silicon Nitride Artefacts

T. A. Stolarski, E. Jisheng, D. T. Gawne & S. Panesar

Brunel University, Uxbridge, Middlesex UB8 3PH, UK

(Received 9 November 1994; accepted 18 January 1995)

**Abstract:** The results of studies on the influence of load and abrasive particle size on the rate of material removal from the surface of a silicon nitride ball are presented and discussed. They indicate that there is an optimum size of abrasive particle at which the material removal rate is at its maximum. The same is true, but to a lesser extent, with the effect of load.

## 1 INTRODUCTION

Ceramic materials are known for their wear resistance which is reflected by the notoriously low material removal rates in grinding by conventional methods. These methods contribute substantially to the final cost of ceramic balls which is thus much higher than that of steel balls. Primarily, they are processed by sintering and hot isostatic pressing (HIP) of ceramic powders. The sintering results in shrinkage, affecting the roundness of balls, which has to be corrected by grinding during the first stage of the finishing process. The surface skin of 100–200  $\mu\text{m}$  thickness is compositionally and microstructurally different from the core of the ball due to reactions with the environment during sintering. The skin has then to be removed during the second stage of finishing. Finally, the surface finish required for ball bearing applications is attained by the third finishing stage. Typical ball bearings of diameter in the range of 6–15 mm are required to be round to within 0.1 mm and to have surface roughness of 0.005–0.01  $\mu\text{m}$   $R_a$  value.<sup>1</sup>

The three stages of finishing are carried out by diamond abrasive lapping, each stage distinguished only by the coarseness of the abrasive particles. A typical finishing process uses two circular cast iron plates placed face to face with concentric matching grooves cut in them. Balls are

fed into the grooves and are forced to roll by rotation of the plates. The contact geometry ensures that the rolling is accompanied by a spinning motion and microslip which is considered as responsible for material removal. Also, the steady motion of the balls could result in tracks developing on them. Hence, in order to secure uniform material removal the motion of the ball is interrupted by returning it to a hopper. When the ball enters the process again its orientation is randomised with respect to its previous pass. A typical batch of balls in the 6–15 mm diameter size range may be in the high hundreds, with 10% between the laps at any time. Total processing time may be several weeks, although any one ball may be actively processed for only 30–50 h. Typically, material removal rates of 0.1–0.2  $\mu\text{m}/\text{min}$ , loads per ball of tens of Newtons, and the relative speeds of rotation of 400 mm diameter lapping plates of 50 rpm are attained. It is obvious that the current practice in grinding ceramic materials is painfully slow and, therefore, expensive. In order to improve this unsatisfactory state of affairs, a number of studies into the grinding of engineering ceramics have been carried out.<sup>2–5</sup> The main objective of the study reported here is to ascertain which of a number of potentially useful tribological processes is the most effective in material removal. Equally important is to determine what damage, if any, is inflicted on the subsurface

region of a ceramic element during accelerated material removal. The study reported in this paper concerns the first stage of the research programme and aims to identify the mechanisms of material removal and to relate them to the effectiveness of grinding process when different loads and abrasive particle sizes are used.

## 2 EXPERIMENTAL

### 2.1 Apparatus

All results presented in this paper were obtained from the tests on a model contact created by the well known four-ball configuration. The details of the apparatus used are described elsewhere.<sup>6</sup> In normal configuration, the top ball is located in a holder carried by vertically mounted spindle and is rotated in a loaded contact with three other balls which are free to rotate in a specially shaped cup. In the study reported here, the top ball was replaced by a cone made of stainless steel and placed in contact with nine 6.8 mm nominal diameter silicon nitride balls. The cup and the cone were fabricated out of 304 grade stainless steel. The cone together with the spindle was driven by an electronically controlled electric motor. In this way each ball was in contact with the cup at two points and with the cone at one point. The configuration called 'three-point contact' is shown schematically in Fig. 1. The balls were manufactured by HIP method mentioned earlier.

### 2.2 Experimental procedure

The experiments were carried out at a rotational velocity of the spindle ranging from 1500 to 7500 rpm. The normal loads on the set of nine balls ranged from 200 to 4000 N. For most of the experiments, oil-based diamond slurries of particle size ranging from 1 to 45  $\mu\text{m}$ , supplied by Kemet Ltd, were used. Additional experiments were also carried out during which diamond paste of 45  $\mu\text{m}$  particle size added to the standard brake fluid was

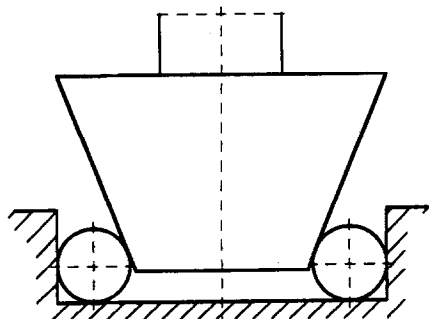


Fig. 1. Three point contact configuration used during grinding experiments.

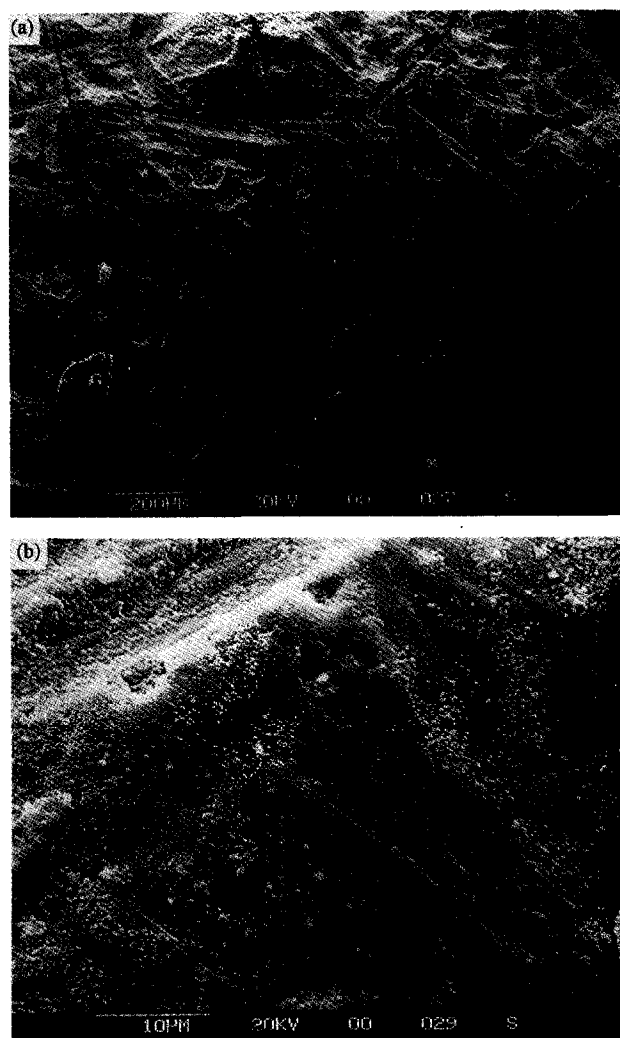


Fig. 2. The appearance of ball surface before the grinding experiment: (a) magnification  $\times 100$ ; (b) magnification  $\times 2000$ .

used. In general, 3 ml of oil-based slurry was placed in the cup which was then covered with a lid to stop spillage. Each experiment lasted 60 min and was repeated three times in order to determine the variability in the results. A satisfactory repeatability of test results was found, however, the number of test repeats did not warrant any statistical analysis.

The silicon nitride blank balls, in the as-received condition, had very rough surfaces of the order of 100–200  $\mu\text{m}$   $R_a$  and contained many surface imperfections. Figure 2 shows an SEM micrograph of the blank ball surface taken at magnification of 100 and 2000. Therefore, each ball before testing was subjected to a run-in process to remove these imperfections. Running-in was carried out in the following way: 0.5 g of 15  $\mu\text{m}$  diamond paste was smeared onto the set of blank balls and 3 ml of an oil-based slurry of 15  $\mu\text{m}$  diamond particle size was added into the cup. Initially, the set of 9 blank balls was loaded at 100 N and rotational velocity of 700 rpm applied for 1 h. Then, the load was increased to 200 N and the rotational velocity

increased to 3000 rpm. At this velocity and load, the balls were run-in for 2 h during which approximately 300  $\mu\text{m}$  of the material was removed from each ball resulting in the average reduction of their diameters from the initial 6.8 mm to 6.5 mm.

After running-in, all balls were cleaned ultrasonically and their diameter measured with a micrometer. Before the experimental run, the cup as well as the balls and the cone were thoroughly cleaned to ensure that the conditions before each test were nominally the same. The balls were placed in the cup and a fresh measure of a grinding fluid with nominally the same amount of abrasive particles was added into the cup. The required velocity and load were set and the experiment was run for 60 min. At the end of experiment, the balls were removed from the cup, ultrasonically cleaned and their diameters measured with a precision micrometer. The average changes in diameter were recorded and the rate of material removal per unit time was calculated. Further post-test studies were carried out on balls representing all used test conditions. These studies involved SEM ball surface studies, and wear debris analysis. In order to determine whether the grinding inflicted any subsurface damage some balls were cut in half, cross-section polished and studied under the light microscope and the scanning electron microscope. In order to ensure that the material removal rate measured truly reflects the action of a particular abrasive particle size, a separate cup and cone were used for every particle size used during the studies.

### 3 RESULTS FROM MODEL GRINDING EXPERIMENTS

#### 3.1 The effect of load and abrasive particle size

All experiments investigating the effect of load were carried out at a constant speed of 3000 rpm. Grinding fluids consisting of oil-based diamond slurries of particle size ranging from 1 to 45  $\mu\text{m}$  were used. The diamond particles in these slurries were homogeneously mixed and suspended in kerosene-type oil-based solution. The load on a set of 9 balls was varied from 200 to 4000 N. The run-in balls were placed in the cup and 3 ml of the diamond slurry of known particle size was added to it. The experiment was then started at a known load, constant rotational speed of 3000 rpm and run for 60 min. The material removal rate and the temperature within the cup were measured at the end of each experiment. The temperature within the cup was measured using an Fe-Co thermocouple connected to a digital meter. It reflected a temperature of the

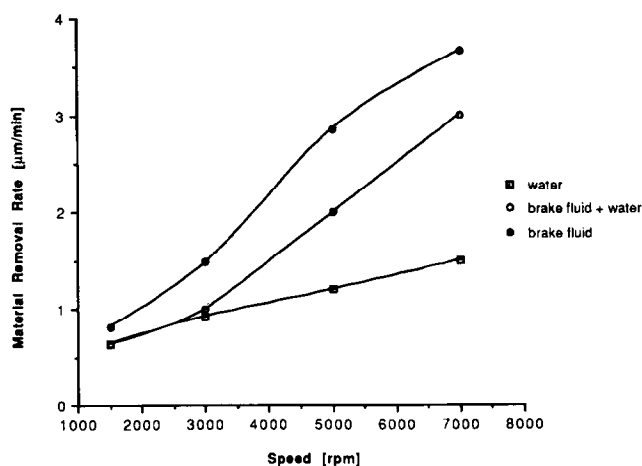


Fig. 3. Material removal rates as a function of speed in different fluids. Composition of grinding slurry: 0.5 g of 45  $\mu\text{m}$  diamond paste in 3 ml fluid. Load — 200 N. Test duration — 1 h.

slurries but not the surface of the ceramic balls.

Figure 4(a) shows the material removal rate plotted against the applied load as a function of the particle size of an oil-based diamond slurry whilst Fig. 4(b) presents the material removal rate as a function of abrasive size for different loads used. For the 1  $\mu\text{m}$  particle size diamond slurry, only a small quantity of the material is removed (removal rate 0.13  $\mu\text{m}/\text{min}$ ) at 200 N load and further increase in the load (from 200 to 4000 N) results in a small gradual increase in the material removal rate (0.4  $\mu\text{m}/\text{min}$ ). However, the surface finish of the balls has been much improved as compared with that produced by running-in. Increasing the particle size from 1  $\mu\text{m}$  to 6  $\mu\text{m}$  alters the material removal rate significantly. For the 6  $\mu\text{m}$  particle size, the material removal rate changes only slightly (from 0.66 to 0.74  $\mu\text{m}/\text{min}$ ) when the load is increased from 200 to 1200 N. However, further increase in the load to 2000 N for this particle size results in the five-fold increase in the removal rate to 3.34  $\mu\text{m}/\text{min}$ . A further rise in the load to 4000 N does then produce a slight increase in the material removal rate. The main trend is that as the load is initially increased, the material removal rate remains approximately constant until a critical load, characteristic for a given abrasive particle size, is reached. Then the material removal rate increases 2–3 times. This indicates a transition from a low material removal rate to a high removal rate.

In comparison with the removal rate at 1  $\mu\text{m}$  particle size, the material removal rate characteristic for 6  $\mu\text{m}$  particle size increases five-fold at lighter loads (200–1200 N) and ten-fold at heavier loads (1600–4000 N). Increasing the particle size from 6–15  $\mu\text{m}$  results in a four-fold increase in the material removal rate at lighter loads (200–1200

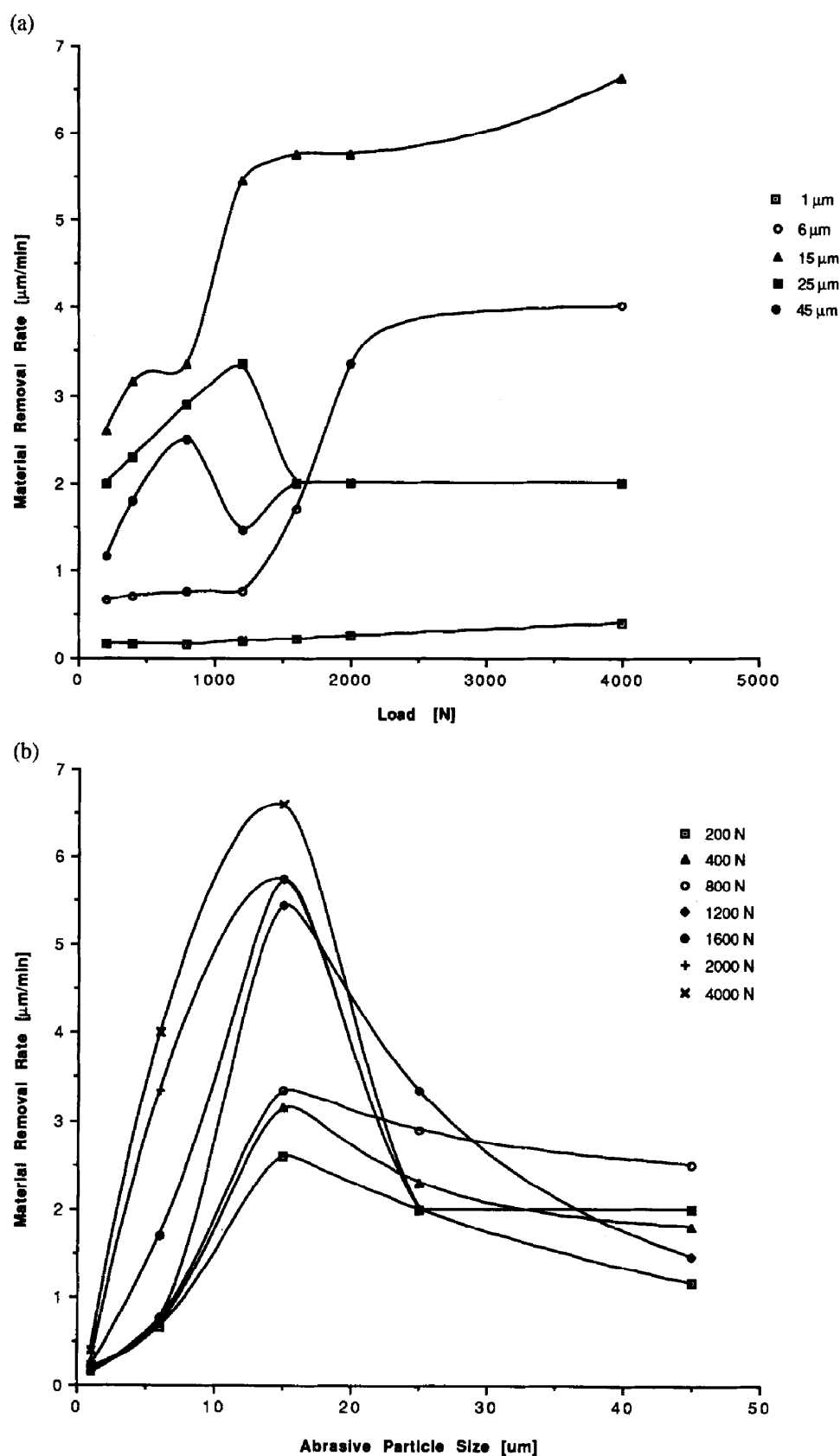


Fig. 4. (a) Material removal rate as a function of load for different abrasive particle sizes. Speed — 3000 rpm. Test duration — 1 h. Grinding fluid — 3 ml oil-based diamond slurry. (b) Material removal rate as a function of abrasive particle size for different loads. Speed — 3000 rpm. Test duration — 1 h. Grinding fluid — 3 ml oil based diamond slurry.

N) and the increase in the removal rate of 1.5 times is achieved at heavier loads (1600–4000 N). The 15  $\mu\text{m}$  particle size slurry also produces the same transitional behaviour as shown by the 6  $\mu\text{m}$

particle size slurry. However, the transition point starts at a load of 800 N instead of 1200 N. Further increase in the particle size to 25  $\mu\text{m}$  reduces the material removal rate by 20% at

lighter loads (200–800 N) and by 70% at heavier loads (1200–4000 N). For this particle size, the material removal rate increases by approximately 30% when the load is increased from 200–1200 N. However, further increase in loading to 1600 N results in a decrease of 40% in the material removal rate. Even further increase in loading (2000–4000 N) produces no changes in the material removal rate. For this relatively large particle size (25  $\mu\text{m}$ ), the transition point results in a decrease in the material removal rate instead of increase in the removal rate shown by the smaller particle sizes of 6 and 15  $\mu\text{m}$ . Further increase in the particle size from 25 to 45  $\mu\text{m}$  results in a similar material removal trend. The removal rate decreases by approximately 20% at lighter loads (200–800 N) and the transition point is at 800 N instead of 1200 N.

In general, the material removal rate with respect to load shows two clear trends. Firstly, the initial increase in the load does not change the material removal rate significantly until a certain critical load is reached. Then, the transition is reached when the material removal rate increases two- or three-fold. Once the transition has occurred, the material removal rate is again independent of the load. Secondly, the material removal rate is affected by the particle size of the diamond slurry. The material removal rate increases as the particle size is increased from 1 to 15  $\mu\text{m}$ . Further increase in the particle size from 25 to 45  $\mu\text{m}$  results in reversal of the trend. Thus, it can be concluded that the optimum material removal rate is reached at the 15  $\mu\text{m}$  particle size. Figures 5 and 6 show temperature within the cup plotted against the load and the material removal rate, respectively, for various particle sizes of the oil-based diamond slurries. It is seen from Fig. 5 that the temperature generally increases with increasing load for all the

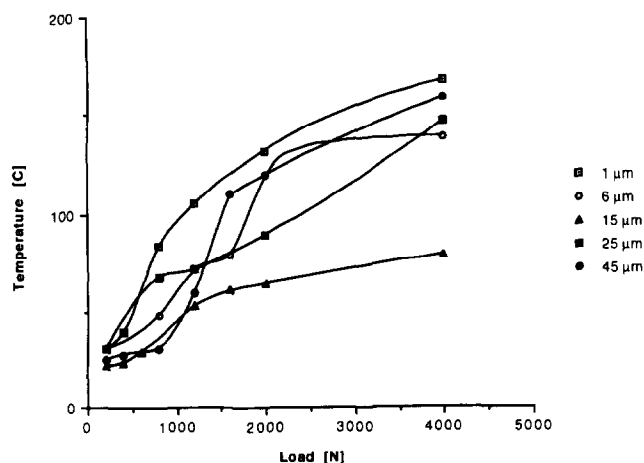


Fig. 5. Temperature of the grinding slurry as a function of load for different abrasive particle sizes. Speed — 3000 rpm. Test duration — 1 h. Grinding fluid — 3 ml oil-based diamond slurry.

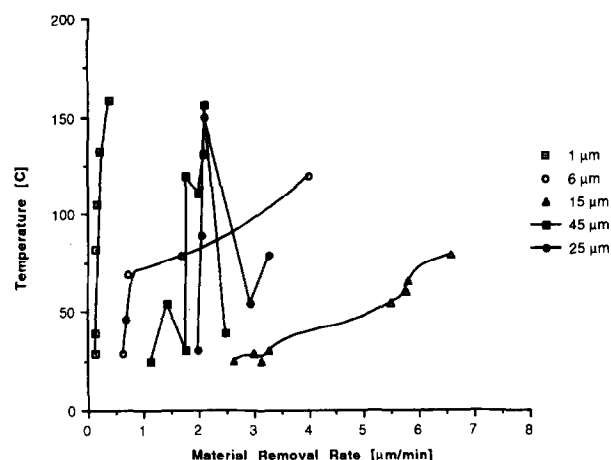


Fig. 6. Temperature of the grinding slurry as a function of material removal rate for different abrasive particle sizes. Speed — 3000 rpm. Test duration — 1 h. Grinding fluid — 3 ml oil-based diamond slurry.

particle sizes. The temperature within the cup is also a function of the particle size at the whole range of loads applied. The temperature decreases from high values to low values as the particle size is increased from 1 to 15  $\mu\text{m}$ .

Figure 6 shows that at 1  $\mu\text{m}$  particle size the temperature within the cup rises sharply with almost negligible change in the material removal rate. The explanation of that observation must be coupled to the enhanced surface finish produced. It is well known that very smooth surfaces can only be produced if some surface plastic deformation is involved. It is believed that a similar process took place during grinding in slurries with 1  $\mu\text{m}$  particles.

For the 6  $\mu\text{m}$  particle size, the temperature rises sharply at the beginning when the material removal rate is very low. Once the transition point is reached the temperature rise is not as dramatic as before and that is accompanied by a steady material removal rate. Also, the surface finish for the 6  $\mu\text{m}$  particle size is not as good as for the 1  $\mu\text{m}$  particle size.

For the 15  $\mu\text{m}$  particle size, the temperature rose steadily while there was a sharp increase in the material removal rate. This sharp increase in the removal rate is an indication of the change of the material removal mechanism and associated with that thermal effects. It is possible that this time the abrasive particles were too large (15  $\mu\text{m}$ ) to pass through the contact zone without being embedded. As a result of that a two body abrasive wear was probably a predominant mechanism of material removal.

For particle sizes of 25 and 45  $\mu\text{m}$ , the temperature versus material removal rate shows a somewhat different behaviour to that described above. Initially, the temperature rises with the removal rate and then, after the transition point, starts to

fall. As it will be seen in the later section, a very coarse surface was produced by 45  $\mu\text{m}$  particles.

The number of diamond particles per unit volume of the slurry could be an important parameter in temperature generation and material removal processes. If  $M$  denotes mass of particles per unit volume of slurry,  $n$  represents number of particles per unit volume and  $m$  is mass of a single particle, then

$$M = nm$$

where  $m$  is given by,

$$m = \frac{4}{3} \pi r^3 \rho$$

In the above expression  $\rho$  is the density of diamond particle and  $r$  its radius. Thus,

$$M = n \frac{4}{3} \pi r^3 \rho$$

or

$$n = \frac{1}{r^3} \left( \frac{3M}{4\pi\rho} \right)$$

For a fixed  $M$  and constant  $\rho$ , and for two particle sizes  $r_1$  and  $r_2$ , the ratio of the number of particles per unit volume is,

$$\frac{n_1}{n_2} = \frac{r_2^3}{r_1^3}$$

and for  $r_1 = 1 \mu\text{m}$  and  $r_2 = 45 \mu\text{m}$ ,

$$\frac{n_1}{n_2} = 91125$$

and so there are approximately 90 000 as many diamond particles per unit volume of slurry for the 1  $\mu\text{m}$  slurry as the 45  $\mu\text{m}$ .

In broad terms, the very large temperature rises for the 1  $\mu\text{m}$  slurry (Fig. 6) could be explained by the very large number of diamond-ceramic ball contacts per unit time which gives rise to a rapid rate of heat generation and accumulation.

In more detail, however, the outcome will also depend upon the operative material removal mechanism. If it is 2-body abrasion for the medium size particles, then the number of embedded diamond particles per unit area of cup surface will accumulate with time which will compensate for their much lower numbers per unit volume and may possibly be related to (or be a cause of) the wear-load transitions in Fig. 4(a). In addition, one unit abrasive action from a medium size particle clearly removes more material than that for a small particle. The question why the removal rates of 25  $\mu\text{m}$  and 45  $\mu\text{m}$  particles at high loads (>2000 N) are lower than those of 15  $\mu\text{m}$  and 6

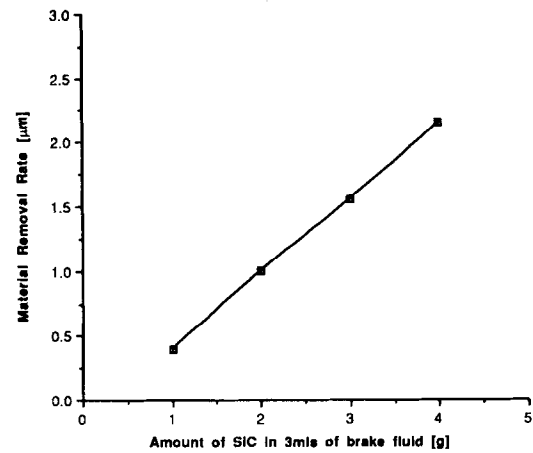


Fig. 7. Material removal rate as a function of abrasive particle concentration in brake fluid. Load — 200 N. Speed — 3000 rpm. Test duration — 1 h.

$\mu\text{m}$  can only be answered in conjunction with the hydrodynamic effects within the cup. As the direct evidence in support of the explanation given below is not available, it must be treated as tentative and hypothetical. The load, speed, and contact configuration created such conditions under which 15  $\mu\text{m}$  particles were able to enter the contact between ceramic balls and the cup and be embedded there because fluid film created by the hydrodynamic action had appropriate thickness. According to test results, these conditions apparently existed for 15  $\mu\text{m}$  particles in the whole range of loads used. However, fluid film thickness created under similar conditions of load, speed and contact configuration must have been too small, especially at high loads (>2000 N), for the 25  $\mu\text{m}$  and 45  $\mu\text{m}$  particles to enter the contact zone. Hence the material removal rates recorded are significantly lower than those for 15  $\mu\text{m}$  particles.

### 3.2 The effect of abrasive particle concentration

Silicon carbide particles of 240 grit size were suspended in the brake fluid solution by the addition of 1% Trinton surfactant. Then 3 ml of the resulting slurry was added to the cup containing a set of 9 run-in silicon nitride balls. Experiments were run for 1 h at 200 N load and 3000 rpm rotational velocity. The concentration of the silicon carbide particles was varied and the results are shown in Fig. 7. It is clearly seen that the concentration of the abrasive particles increases linearly the material removal rate.

## 4 POST-GRINDING STUDIES

### 4.1 Surface of the ball

Microscopy studies were carried out to examine ball surfaces after grinding experiments. SEM

examination of ball surfaces produced under low load (200N) and relatively high speed (3000 rpm) revealed a large number of spots (see Fig. 8). This surface appearance is characteristic for all abrasive particle sizes used. More details about the nature of these spots is provided by micrographs taken at a higher magnification and shown in Fig. 9. They appear to be isolated from each other which points to the supposition that they were created as a result of an indentation either by abrasive particles rolling through the contact zone or by abrasive particles embedded into the cup and upper test piece over which ceramic balls rolled. As it is seen from Fig. 4, material removal rate for fine abrasive particles (1  $\mu\text{m}$ ) does not change in any appreciable way with the load but ball surface finish is usually very good. A typical appearance of ball surface after grinding in the presence of 1  $\mu\text{m}$  abrasive particles is shown in Fig. 10. It is evident that the surface is covered with very fine scratches indicating ploughing on a micro-scale.

Figure 11 shows a typical appearance of the ball surface after grinding characterised by high material removal rate. Deep scratches visible on the surface point to an abrasive wear mechanism, although

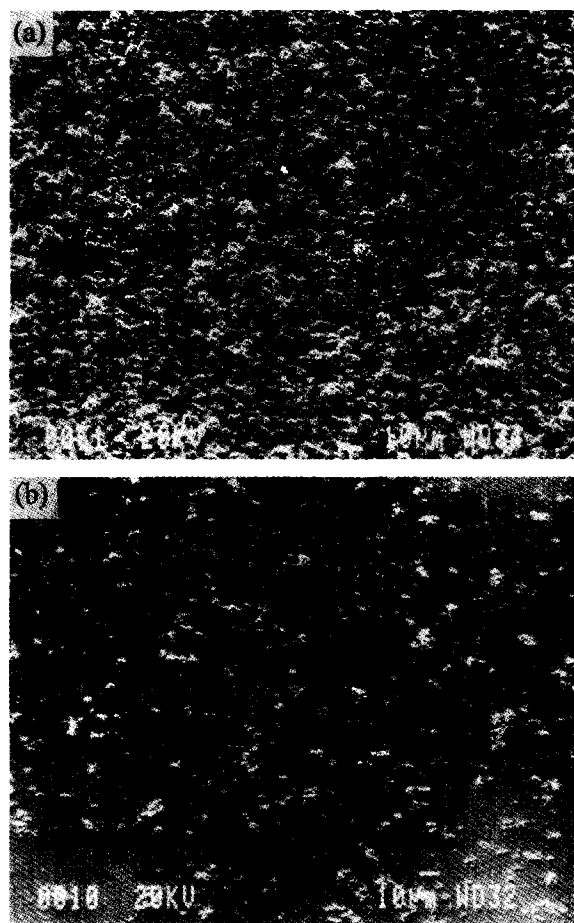


**Fig. 8.** Appearance of ball surface after grinding experiment under 200 N and speed of 3000 rpm: (a) Oil-based slurry containing 25  $\mu\text{m}$  abrasive particles, (b) oil-based slurry containing 1  $\mu\text{m}$  abrasive particles.

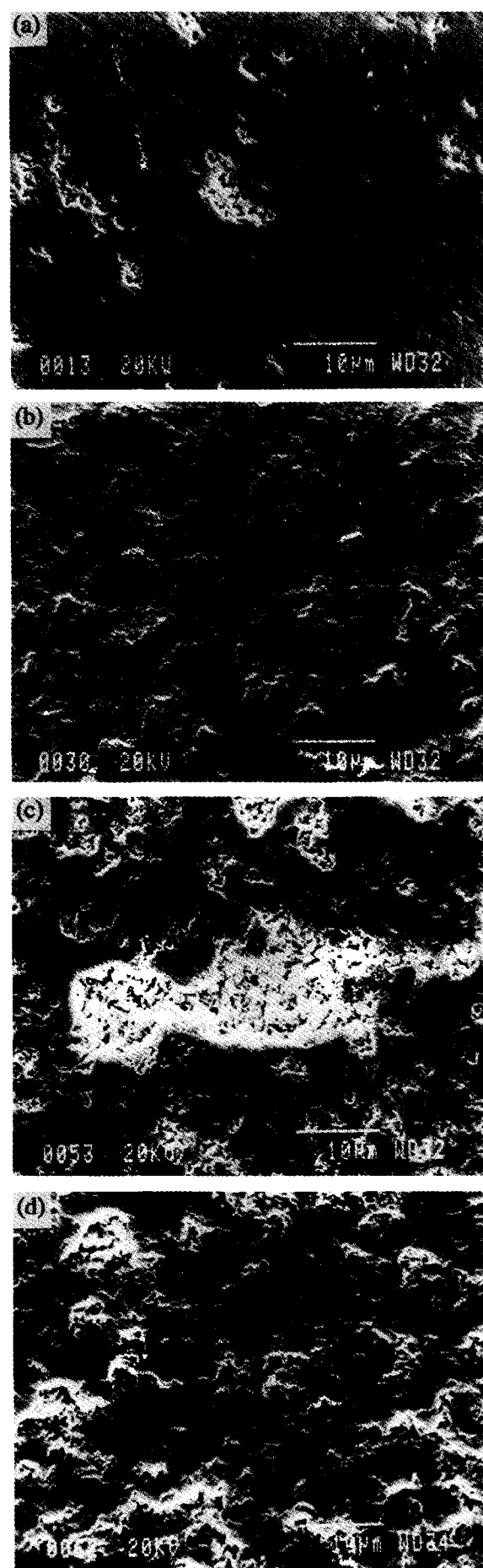


**Fig. 9.** Appearance of ball surface after grinding experiments in slurries containing different abrasive particle sizes. Load — 200 N. Speed — 3000 rpm: (a) 1  $\mu\text{m}$ ; (b) 6  $\mu\text{m}$ ; (c) 15  $\mu\text{m}$ ; (d) 25  $\mu\text{m}$ .

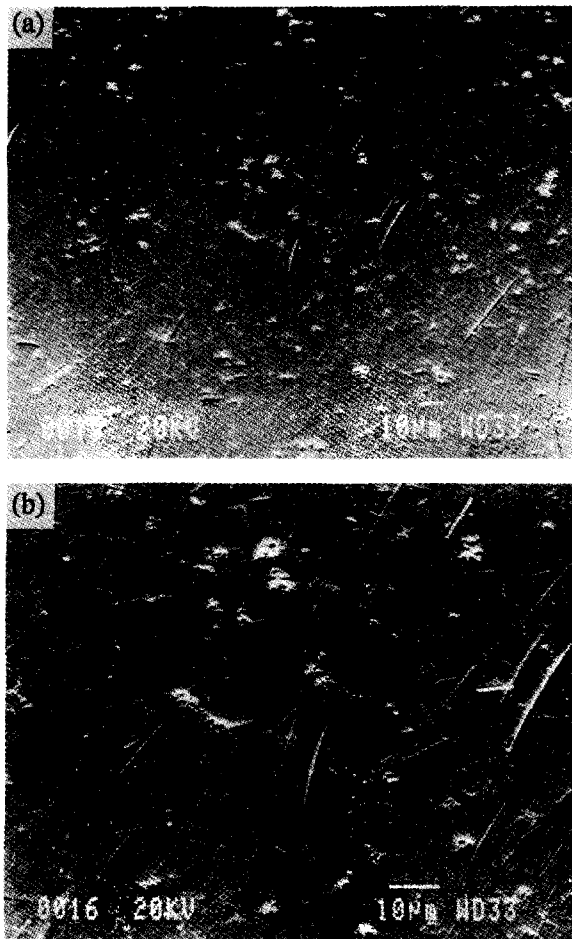


Fig. 10. SEM micrographs of the ball surface after grinding experiment in oil-based slurry containing  $1\ \mu\text{m}$  abrasive particles. Load — 400 N. Speed — 3000 rpm: (a)  $\times 400$ ; (b)  $\times 1000$ .

a brittle fracture could also have been involved in the material removal process to some extent.

Figure 12 shows SEM micrographs of the surface after grinding carried out at the load of 1600 N and abrasive particle size of  $25\ \mu\text{m}$ . This surface appearance is typical for grinding experiments carried out at high loads (up to 4000 N) and in the presence of large abrasive particles ( $25\ \mu\text{m}$  and  $45\ \mu\text{m}$ ). It appears from Fig. 12 that severe damage involving fracture was inflicted on the surface. It seems, therefore, that a major mechanism of grinding was brittle fracture resulting in removal of relatively large fragments of material. Unfortunately, this was not converted into a high material removal rate (see Fig. 4). The probable reason for that is the much lower frequency of fracture events leading to material removal for  $25\ \mu\text{m}$  and  $45\ \mu\text{m}$  particles compared to those events involving two-body abrasion.

#### 4.2 Cross section of the ball

A set of balls representing the range of testing conditions adopted was selected. The balls were cut, cross sectioned, carefully polished and pre-

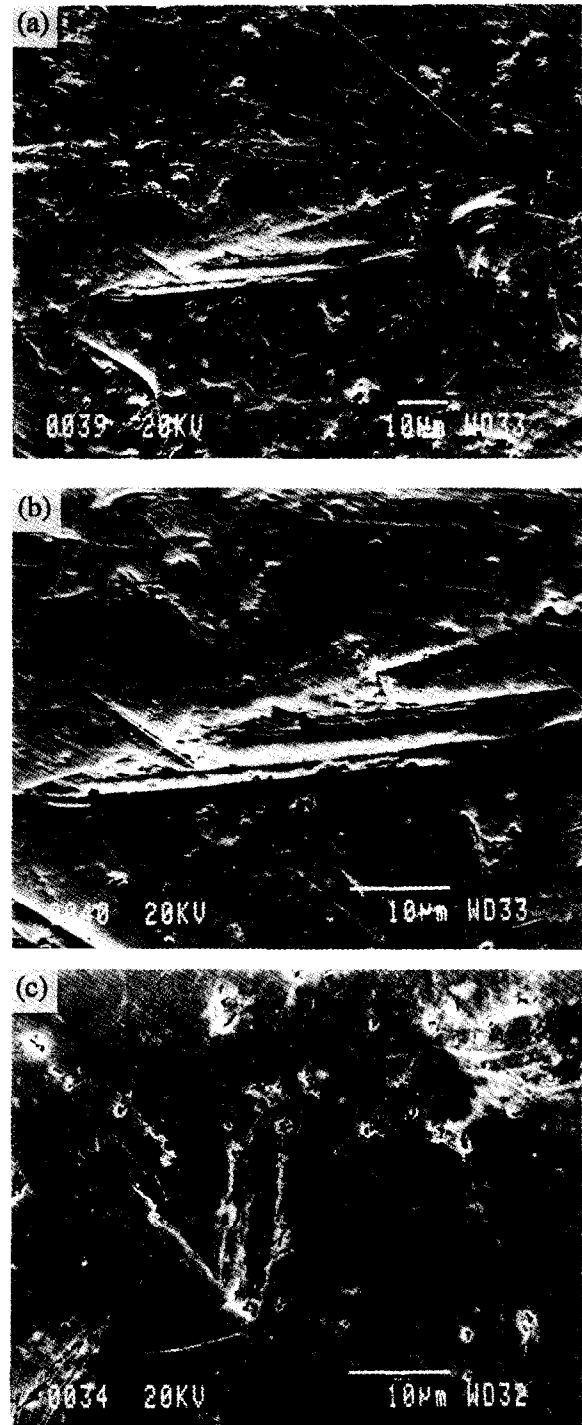


Fig. 11. A typical appearance of the ball surface after grinding in slurry containing  $15\ \mu\text{m}$  abrasive particles characterised by high material removal rate. Load — 1500 N; Speed — 3000 rpm: (a)  $\times 1000$ ; (b)  $\times 2000$ ; (c)  $\times 5000$ .

pared for microscopy studies. The main objective of these studies was to determine how much damage, if any, was incurred by the subsurface region of the ball during grinding. The results are shown in Fig. 13. Careful examination of the micrographs reveals that no damage to the subsurface region was done during grinding experiments except that carried out under heavy load and large abrasive particle size. Figure 14 illustrates the damage sustained by the subsurface region.



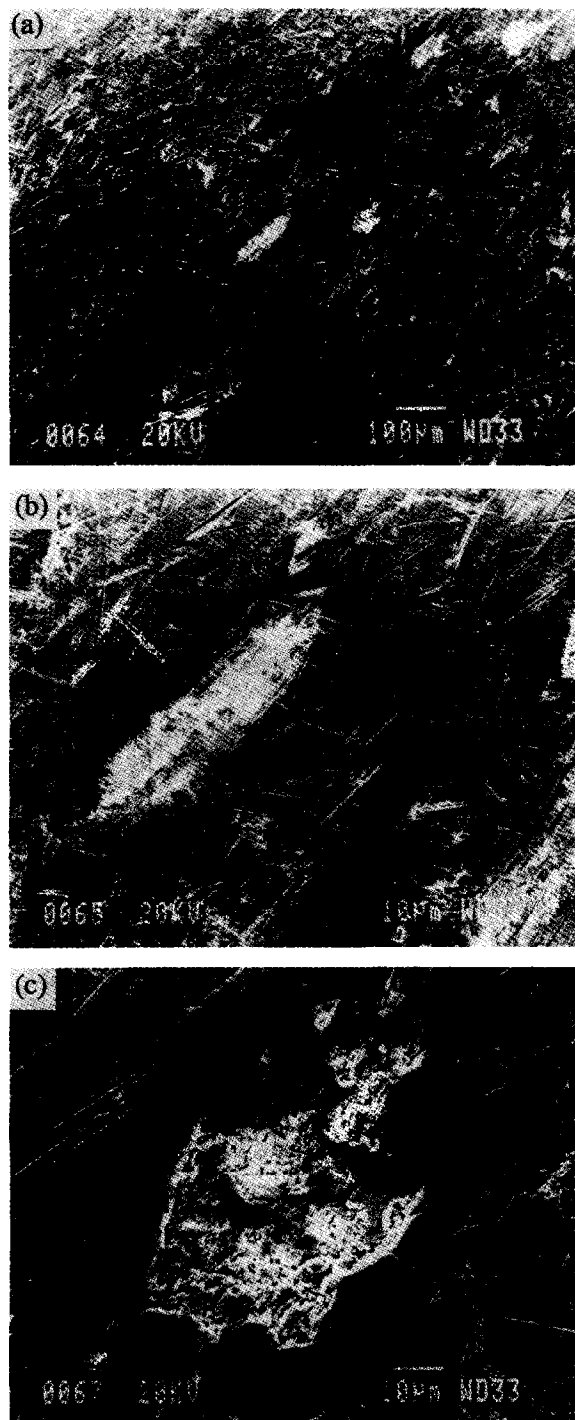


Fig. 12. SEM micrographs of the ball surface after grinding experiment carried out at the load of 1600 N and 25  $\mu\text{m}$  abrasive particle size. Magnification —  $\times 1000$ .

It is seen from Fig. 13 that grinding in the presence of very fine abrasive particles (1  $\mu\text{m}$ ) resulted in a very smooth and even surface. This is also true, to a lesser extent, in the case of grinding under light loads and medium size abrasive particles (15  $\mu\text{m}$ ). However, grinding under high loads and large abrasive particles produced an uneven surface. The surface roughness was assessed quantitatively by measuring the length of the surface profile in a cross section of a specimen and dividing it by the length of a perfect circular arc over

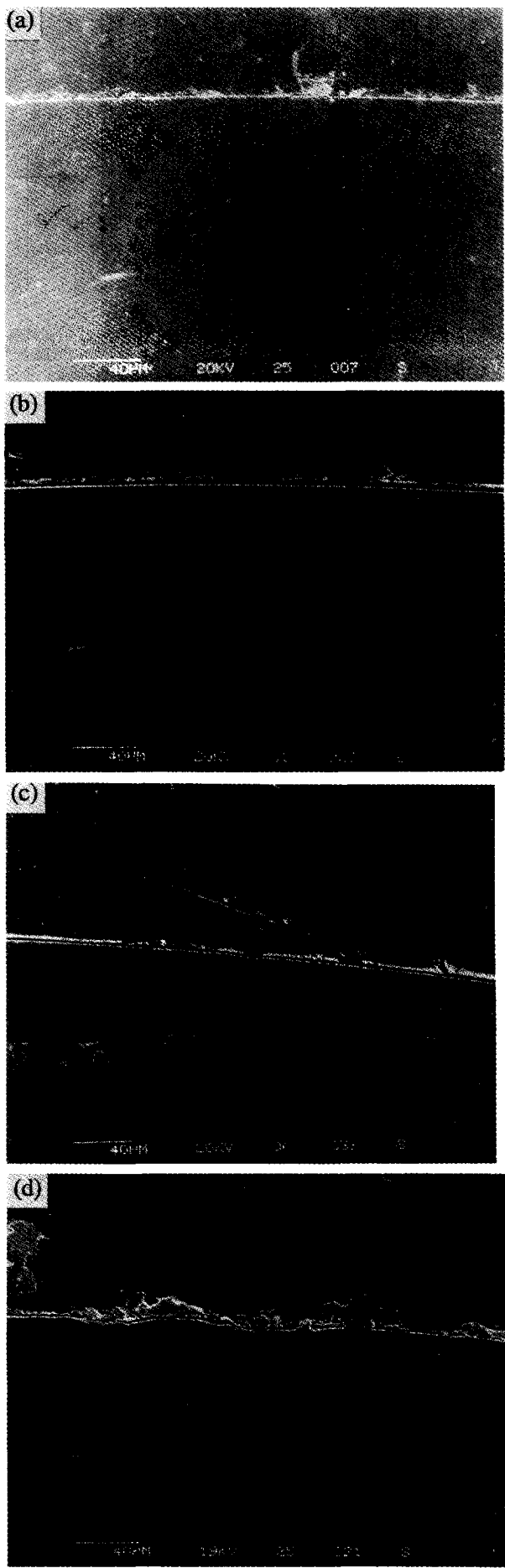


Fig. 13. Surface profile resulting from cross section of balls ground under different test conditions. (a) 1  $\mu\text{m}$ ; (b) 6  $\mu\text{m}$ ; (c) 15  $\mu\text{m}$ ; (d) 25  $\mu\text{m}$ .

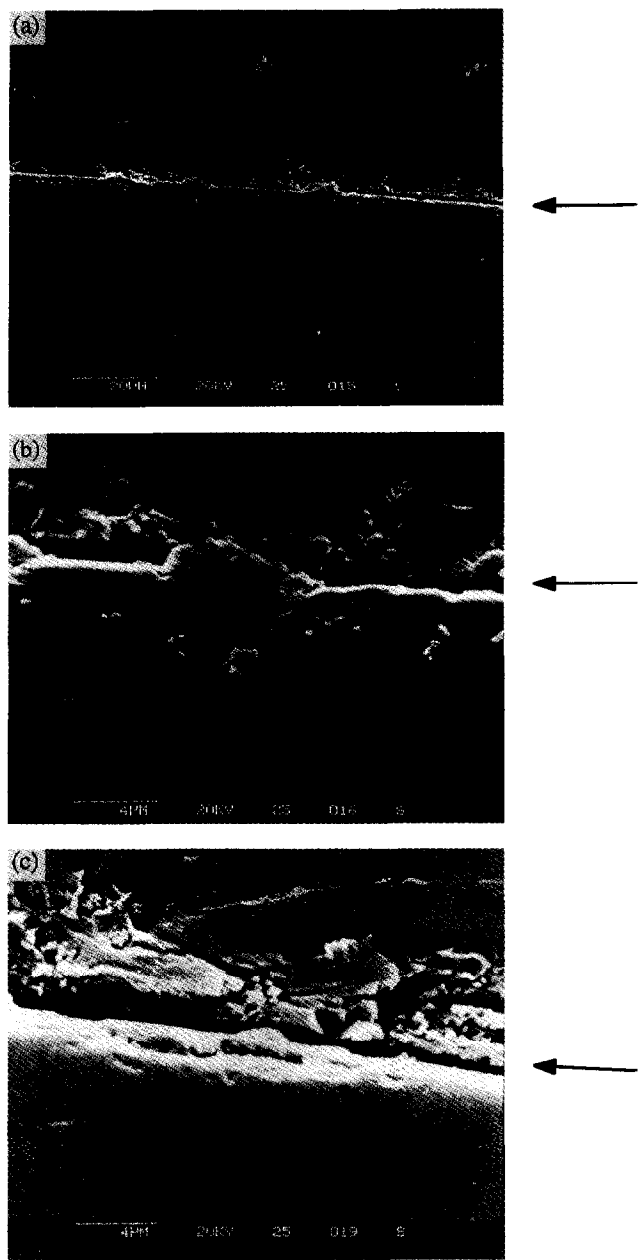


Fig. 14. Damage sustained by the subsurface region of the ball during grinding experiment carried out at the load of 2000 N in 25  $\mu\text{m}$  oil-based slurry.

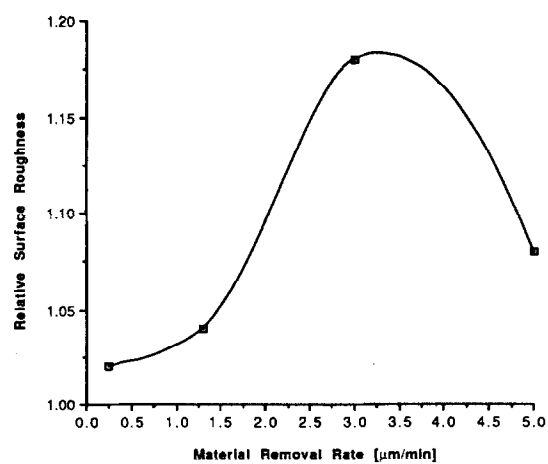


Fig. 15. Relative surface roughness as a function of material removal rate.

the same angular distance. The results are shown in Fig. 15 and can be taken as a measure of surface quality associated with a particular material removal rate achieved under test conditions used.

### 4.3 Debris analysis

Wear debris produced during grinding experiments were collected for further analysis. As expected, it was found that the debris contained not only silicon nitride particles but also diamond abrasive particles and pieces of stainless steel detached from the cup and the cone. All collected debris were subjected to the same separation process with the objective to isolate silicon nitride particles. However, the result of this operation depended on the size of abrasive particles used. For example, it was not possible to completely separate metal debris from silicon nitride debris in the case of 1  $\mu\text{m}$  abrasive particles although it was easier in the case of larger abrasive particles. This must have influenced the elemental analysis of wear debris which was carried out using the energy dispersive spectroscopy attachment in the scanning electron microscope.

Figure 16 shows the spectrum of debris produced during grinding in 1  $\mu\text{m}$  oil-based slurry under the load of 200 N. It is clearly seen that the peak representing iron is very strong. Further analysis by wavelength dispersive spectroscopy revealed that silicon was almost absent in the dot map of elements contained in the debris. Figure 17 shows the appearance of debris collected after grinding experiment carried out at the load of 200 N in 1  $\mu\text{m}$  oil-based slurry. It was rather difficult to separate a single particle as the debris tend to form clusters but the size of the single wear particle is approximately 200–300 nm.

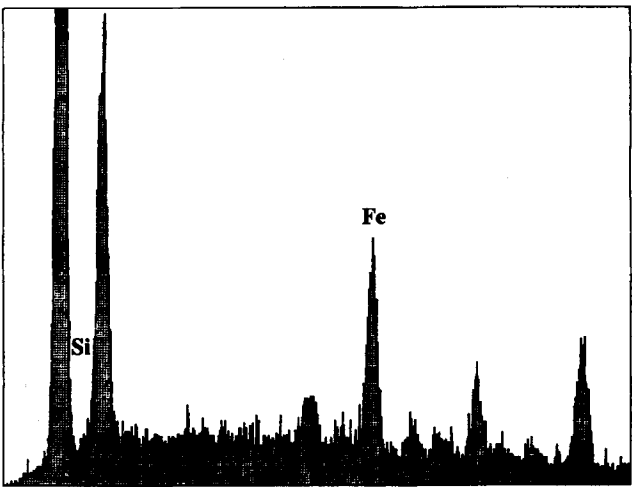


Fig. 16. Elemental analysis of the debris produced during grinding experiment in 1  $\mu\text{m}$  oil-based slurry and under the load of 200 N.

Microscopy examinations of the debris collected after experiments conducted in the presence of 15  $\mu\text{m}$  abrasive particles or under high load (4000 N) and 45  $\mu\text{m}$  abrasive particles showed significantly larger sizes of debris than those produced by grinding conducted in the presence of 1  $\mu\text{m}$  abrasive particles (see Fig. 18). This is in line with the fact that material removal rates obtained for 15  $\mu\text{m}$  abrasive particles were high and is reflected in the sizes of wear debris.

Figure 19 shows the results of elemental analysis of wear debris produced by grinding at the load of 1600 N in 15  $\mu\text{m}$  oil-based slurry. It is clearly seen that the silicon peak is strong while the iron peak is hardly visible which, again, reflects the results of the separation process described earlier. Subsequent analysis using wavelength dispersive spectroscopy confirmed the presence of a substantial quantity of silicon in the debris. This finding is indicative of the high material removal rate characteristic for grinding in the presence of 15  $\mu\text{m}$  abrasive particles.



Fig. 17. Appearance of debris collected after grinding experiment carried out at the load of 200 N in 1  $\mu\text{m}$  oil-based slurry.

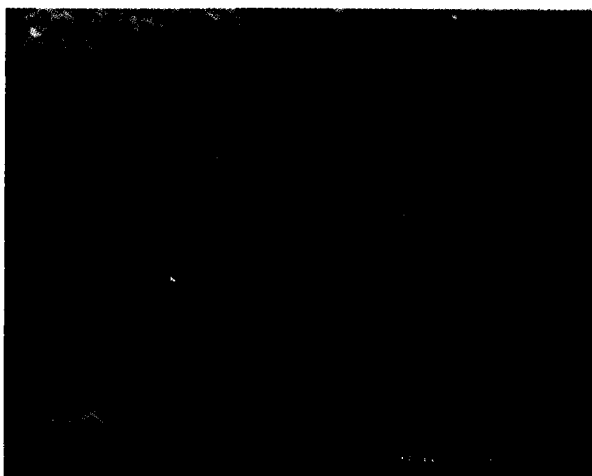


Fig. 18. Appearance of debris resulting from grinding in the presence of large abrasive particles (45  $\mu\text{m}$ ) and heavy load (4000 N).

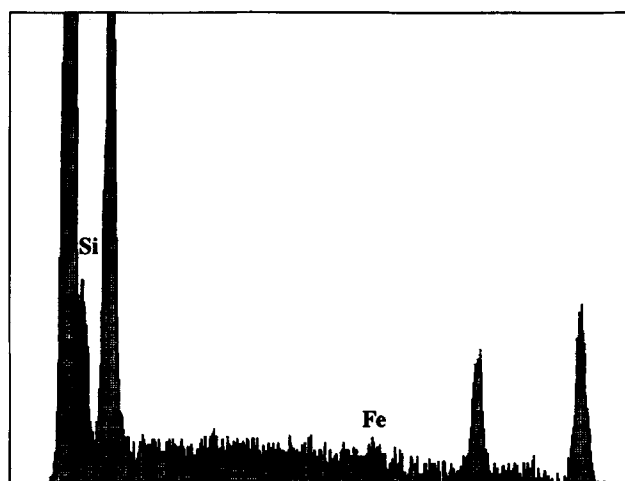


Fig. 19. Elemental analysis of the debris produced by grinding at the load of 1600 N in 15  $\mu\text{m}$  oil-based slurry.

## 5 CONCLUSIONS

Results presented in this paper justify the following conclusions:

- (i) The material removal rates recorded during model grinding of silicon nitride balls strongly depend on the mechanism of interaction between ball surface and an oil-based diamond slurry.
- (ii) The highest rate of material removal occurred in the presence of 15  $\mu\text{m}$  abrasive particles where the predominant mechanism was apparently abrasive wear.
- (iii) The abrasive particle size and the load influence the rate of material removal and the specific combination of those two factors leads to an optimal removal rate.
- (iv) The quality of surface finish of ceramic balls seems to be linked to the rate of material removal. The surface roughness increases with increasing material removal rate reaching a peak value at a removal rate of 3.5  $\mu\text{m}/\text{min}$ . Afterwards the opposite trend seems to be valid.
- (v) Material removal during grinding in slurry containing large abrasive particles (45  $\mu\text{m}$ ) and under relatively high loads (4000 N) appears to take place by brittle fracture resulting in subsurface cracks in the ceramic ball.

## ACKNOWLEDGEMENTS

The authors would like to thank the Science and Engineering Research Council and the Defence Research Agency, who are funding the research, for permission to publish this paper.

**REFERENCES**

1. CUNDILL R. T., Commercial application of precision manufacturing at sub-micron level. *SPIE Proceedings Series*, Vol. 1573 (1991) pp. 76–86.
2. STOLARSKI T. A., Accelerated wear of ceramic balls. *Ceramic Int.*, **18** (1992) 379–438.
3. KATO K. & UMEHARA, N., A study on magnetic fluid grinding. *Trans. JSME*, **54** (1988) 27–31.
4. KIM T. J., GIELISS, P. J. & SHORT, J. F., Wear of diamond particles for grinding ceramics. *Int. J. Prod. Res.*, **22** (1984) 565–74.
5. FREI, H. & GRATHWOHL, G., Microstructure and strength of advanced ceramics after machining. *Ceram. Int.*, **19** (1993) 93–104.
6. LAWRENCE C. C. & STOLARSKI, T. A., Rolling contact wear of polymers. *Wear*, **132** (1989) 183–91.